

SUPPORTING INFORMATION

ANCIENT AND MODERN MECHANISMS COMPETE IN PROGESTERONE RECEPTOR ACTIVATION

Sabab H. Khan¹, Namita Dube¹, Nishanti Sudhakar¹, Olivia Fraser¹, Priscilla Villalona¹, Sean M. Braet², Stephanie Leedom¹, Erin R. Reilly¹, Jacob Sivak², Kenidee Crittenden², C. Denise Okafor^{1,2*}

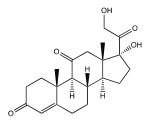
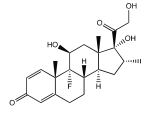
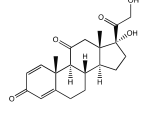
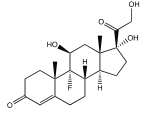
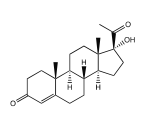
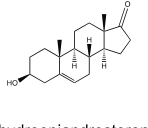
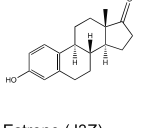
¹Department of Biochemistry and Molecular Biology, Pennsylvania State University, University Park, PA, 16802, USA

²Department of Chemistry, Pennsylvania State University, University Park, PA, 16802, USA

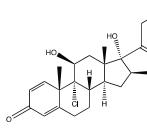
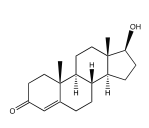
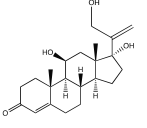
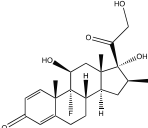
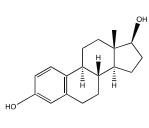
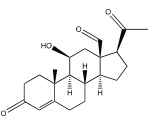
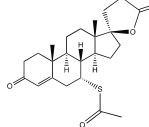
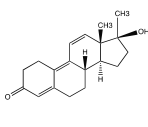
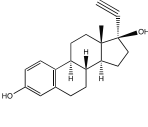
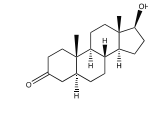
*Email: cdo5093@psu.edu

Figure S1. Structures, names and 3-letter symbols of the steroidal ligands used in the study

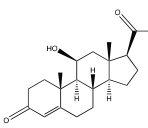
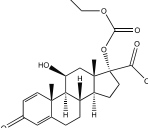
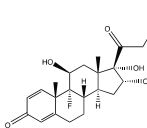
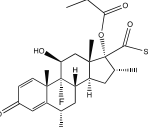
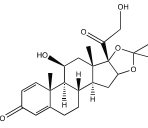
Inactive ligands

				
Cortisone (PD0)	Dexamethasone (DEX)	Prednisone (PDN)	Fludrocortisone (ZK5)	17-alpha-hydroxyprogesterone (17A)
				
Dehydroepiandrosterone (AND)	Estrone (J3Z)			

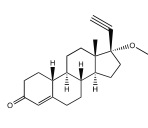
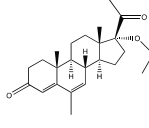
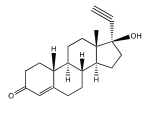
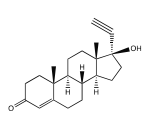
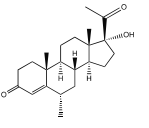
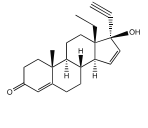
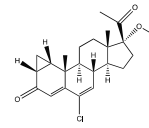
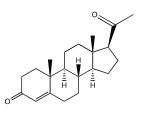
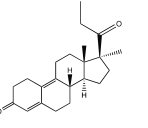
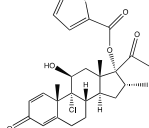
Weak potency ligands

				
Beclomethasone (BLX)	Testosterone (TES)	Cortisol (HCY)	Betamethasone (BM0)	Estradiol (EST)
				
Aldosterone (AS4)	Spironolactone (SNL)	R1881 (R18)	17-alpha-ethinyl-estradiol (3WF)	Dihydrotestosterone (DHT)

Moderate potency ligands

				
Corticosterone (COR)	Loteprednol etabonate (LE8)	Triamcinolone (1TA)	Fluticasone propionate (FLP)	Budesonide (BUD)

High potency ligands

				
Norethindrone acetate (ND0)	Megestrol Acetate (MUZ)	Norethindrone (NDR)	Ethisterone (ET0)	Medroxyprogesterone (MP0)
				
Gestodene (GE0)	Cyproterone acetate (CA4)	Progesterone (STR)	Promegestone (P0M)	Mometasone furoate (MOF)

Ligands	3 letter symbol	EC ₅₀ values (μM)		
		Reference 1	Reference 2	Reference 3
Cortisone	PD0			>10
Dexamethasone	DEX		4.78	>10
Prednisone	PDN			>10
Fludrocortisone	ZK5			>10
17-alpha-hydroxyprogesterone	17A		>10	
DHEA	AND			>10
Estrone	J3Z			>10
Beclomethasone	BLX		6.30	
Testosterone	TES	6.26	0.05	0.15
Cortisol	HCY	6.16		>10
Betamethasone	BM0		4.78	
Estradiol	EST	3.18	0.91	3.60
Aldosterone	AS4		1.12	0.71
Spirolactone	SNL		0.56	0.94
R1881	R18			0.78
17-alpha-ethinylestradiol	3WF	0.40		
Dihydrotestosterone	DHT		0.39	1.21
Corticosterone	COR		7.20E-02	9.00E-03
Loteprednol Etabonate	LE8	2.00E-02		
Triamcinolone	1TA	6.00E-03	5.88E-02	
Fluticasone Propionate	FLP	4.00E-03		
Budesonide	BUD	3.00E-03		
Norethindrone acetate	ND0	2.00E-03		
Megestrol Acetate	MUZ	1.00E-03		
Norethindrone	NDR	1.00E-03		1.00E+01
Ethisterone	ETO			9.19E-04
Medroxyprogesterone	MPO	4.00E-04		
Gestodene	GEO	3.00E-04		
Cyproterone acetate	CA4		7.90E-04	2.00E-04
Progesterone	STR		3.89E-05	2.50E-03
Promegestone	POM		1.28E-05	2.90E-05
Mometasone	MOF			1.20E-05

Table S1. EC₅₀ values of 32 ligands in this study are derived from **Ref 1:** Fan et al, Toxicological Sciences, 2015. **145**(2): p. 283-295, **Ref 2:** Sedlák et al, Comb Chem High Throughput Screen, 2011. **14**(4): p. 248-66., **Ref 3:** Wilkinson et al, SLAS Discovery, 2008. **13**(8): p. 755-765.

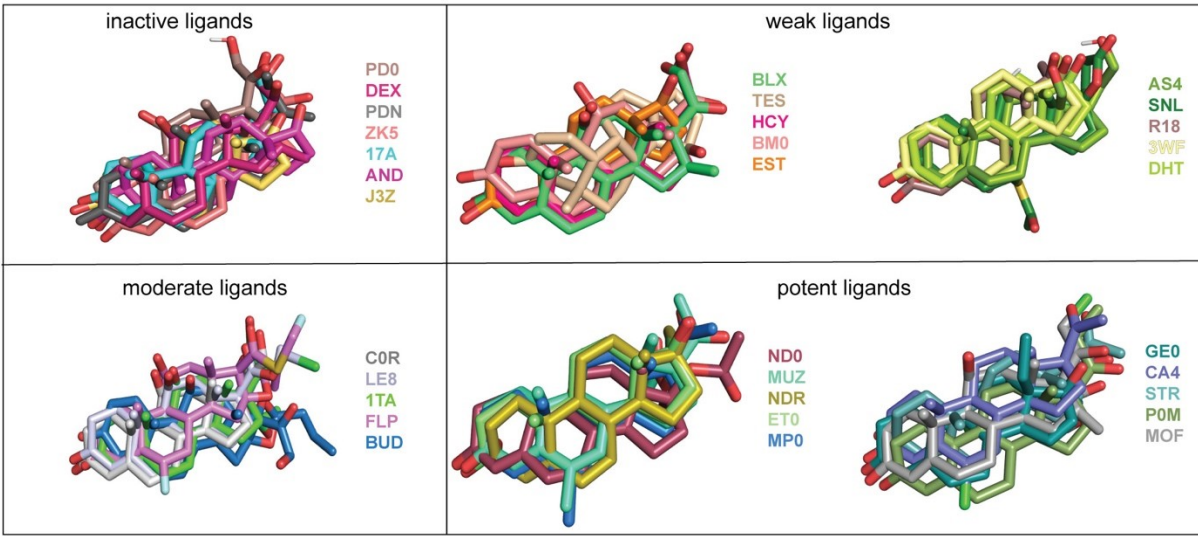
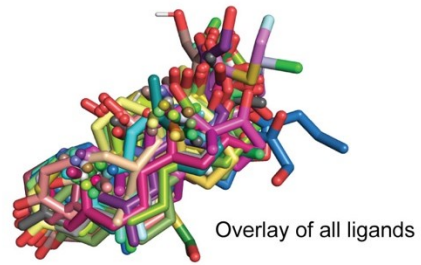
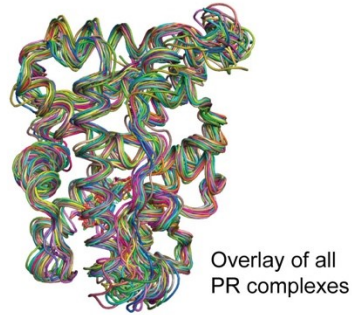


Figure S2. Representative structures of PR-ligand complexes are superposed to reveal binding orientation of steroid hormones. Ligands are also extracted from the complexes and shown separately, grouped by ligand class. All steroidal ligands retain the same orientation and position within the binding pocket.

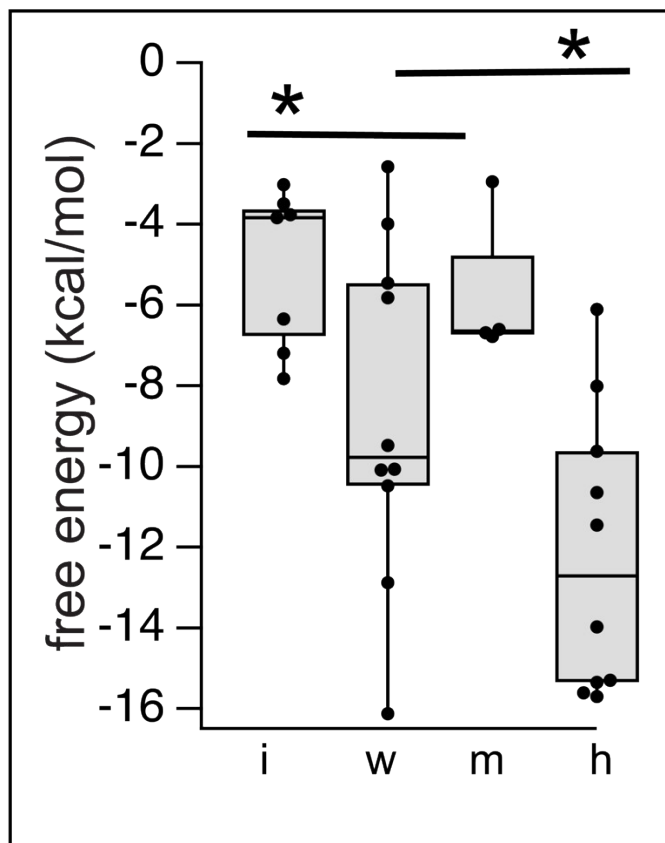


Figure S3. Free energy calculations using MM-PBSA reveal a relationship between potency and binding energy. Compared to all other ligands, inactive ligands and high potency ligands displayed significantly higher and lower free energies respectively. (*, $p < 0.05$ by two-tailed, unpaired t-test)

RE S	F794	L797	L887	C891	V903	F905	M909	I913	N719	M756	L763	R766	F778
17A	23.10 5	21.42 7	13.61 6	13.53 6	28.95 0	25.46 0	4.764	0.136	18.67 8	6.873	2.844	42.23 9	23.77 2
AND	27.55 6	20.41 2	13.91 5	13.58 6	7.899	32.64 1	1.738	5.297	5.001	4.883	5.946	62.38 9	27.75 9
DEX	19.11 1	23.18 9	18.15 2	16.08 7	32.22 6	26.31 4	3.101	-0.177	20.82 8	7.437	3.088	52.60 3	25.25 8
J3Z	18.03 3	18.87 2	13.01 6	13.90 6	15.69 7	33.31 7	2.648	4.507	13.30 3	5.613	3.349	67.03 6	19.11 3
PDN	38.18 2	22.36 7	17.73 5	12.70 0	2.993	21.53 6	-1.172	0.353	-9.962	4.838	3.369	65.83 7	23.43 7
PD0	20.41 6	22.64 5	14.82 2	12.74 3	32.88 6	26.17 7	4.225	-1.111	19.51 2	-0.243	6.214	51.19 6	28.20 6
ZK5	36.38 2	14.49 2	13.22 3	13.65 2	4.895	21.13 1	2.795	0.774	-7.370	0.251	-0.641	55.09 9	18.71 7
TES	32.27 8	16.79 1	15.30 6	12.46 6	9.106	24.62 7	-1.463	-0.198	-1.235	6.244	-1.125	61.87 1	21.11 5
SNL	27.84 2	18.63 7	9.061 2	11.98 2	6.651	22.60 1	2.996	1.432	-4.823	4.105	-7.263	66.47 5	19.12 4
HCY	35.02 1	18.68 3	14.30 5	14.45 4	13.96 0	22.53 7	3.228	0.877	2.688	0.984	-0.278	62.28 1	23.06 5
EST	36.85 9	19.17 3	16.36 3	11.21 5	6.355	24.41 1	-2.776	1.626	-3.090	9.975	-2.183	59.95 5	17.59 2
DHT	28.84 4	20.22 6	14.98 0	13.50 0	10.51 8	27.81 5	0.663	2.544	3.048	5.025	1.147	55.33 6	22.37 3
BM0	38.88 9	23.96 0	13.09 9	16.47 9	5.262	26.45 7	4.291	4.053	-4.884	0.748	6.893	69.00 6	21.25 0
R18	30.47 2	21.44 8	13.60 2	11.66 0	11.22 4	26.16 7	-3.437	0.660	3.624	3.890	-6.410	47.64 0	15.32 9
BLX	27.87 8	21.50 8	16.38 6	15.67 7	13.58 2	27.43 5	-0.178	4.708	1.071	9.190	5.477	56.74 0	22.95 9
AS4	29.90 8	14.61 2	11.66 3	11.05 4	9.160	32.81 2	0.275	2.655	0.727	1.574	2.333	67.38 5	24.33 2
3WF	28.59 4	18.44 1	15.05 1	11.84 8	15.29 0	24.35 4	-2.709	2.046	6.329	8.815	-2.842	61.17 8	16.71 2
1TA	27.90 5	16.86 9	14.04 8	12.31 3	12.86 8	26.55 0	2.294	2.111	0.736	4.841	3.096	50.78 3	23.17 7
C0R	21.02 8	16.56 3	14.14 3	14.39 6	9.349	32.60 0	3.193	3.474	2.968	5.761	2.412	61.58 2	24.24 8
LE8	23.46 4	12.81 3	19.37 3	20.18 3	37.43 9	41.90 0	-0.612	7.609	26.75 4	15.65 1	7.885	60.94 6	25.88 3
BUD	22.77 4	28.63 4	22.48 6	18.69 7	28.86 5	39.79 6	2.322	6.037	18.27 8	10.53 5	11.22 2	61.41 4	29.80 5
FLP	30.04 2	12.95 2	18.52 1	17.78 8	52.01 3	47.98 2	2.615	8.314	42.99 8	14.48 2	2.567	48.88 5	22.21 3
CA4	13.56 0	11.32 2	17.39 0	17.83 6	22.07 4	35.91 4	2.670	3.885	23.70 9	15.79 4	1.911	58.35 2	22.52 3
ET0	23.54 9	35.46 9	12.86 2	13.11 2	3.449	19.12 8	4.297	-2.674	0.545	-3.378	-3.514	47.95 6	17.59 8
GE0	23.66 7	23.95 3	14.30 5	7.129	2.066	16.09 5	-2.753	-4.064	-5.119	-4.481	-8.372	37.64 0	11.01 8
MP0	26.09 4	20.99 5	16.82 6	14.77 3	34.09 7	29.72 1	6.253	1.968	25.10 4	6.118	1.491	58.69 3	23.24 9
NDR	27.28 1	19.21 7	14.56 2	12.64 4	14.41 5	30.62 5	-0.290	4.412	6.602	13.38 1	-7.464	41.19 1	14.59 4
P0M	24.39 8	20.75 3	14.94 7	12.03 2	12.64 2	31.88 0	4.406	2.572	15.31 4	1.114	-4.662	50.61 4	16.50 5
STR	23.72 9	24.13 0	18.17 5	12.60 9	16.13 0	26.72 5	3.207	-2.356	16.12 4	7.607	0.081	62.37 5	21.78 0
ND0	25.82 4	22.74 1	15.67 2	9.768	12.70 0	28.76 4	6.656	7.805	19.39 3	11.58 4	-8.632	47.07 4	15.14 9
MUZ	26.21 3	17.59 4	14.34 0	14.56 4	29.02 8	31.39 9	4.038	2.420	23.93 7	8.654	3.281	61.74 2	22.94 0
MOF	25.13 4	23.31 8	19.34 9	13.96 0	9.912	24.34 8	5.177	2.310	-3.281	1.758	0.657	52.03 8	18.65 0

Table S2: Solvent accessible surface area calculation of binding pocket residues. Ligands are grouped by class (inactive, weak, moderate and high potency). Units are Å².

RES	N719	M756	L763	R766	F778	F794	L797	L887	C891	T894	V903	F905	M909	I913
17A	-0.65	-1.29	-1.01	-0.21	-1.20	-0.07	-1.33	-1.02	-1.30	-0.52	-0.09	-0.77	-0.84	-0.11
PD0	-1.52	-1.54	-1.11	-0.25	-1.23	-0.23	-1.05	-1.13	-1.29	-0.85	-0.31	-0.66	-0.78	-0.12
DEX	-1.76	-1.16	-0.96	-0.17	-0.88	-0.11	-1.49	-1.03	-1.19	-0.98	-0.55	-1.03	-1.01	-0.18
ZK5	-1.68	-1.88	-0.99	-0.12	-1.51	-0.34	-0.93	-1.18	-1.43	-1.32	-0.33	-0.49	-0.66	-0.11
AND	-0.15	-1.38	-1.00	-0.09	-0.90	-0.08	-0.86	-1.41	-1.08	-0.12	-0.06	-0.37	-0.66	-0.17
J3Z	-0.22	-1.24	-1.10	-0.09	-1.43	-0.05	-0.89	-1.27	-1.04	-0.06	-0.02	-0.23	-0.64	-0.12
PDN	-2.26	-1.50	-0.79	-0.24	-1.04	-0.40	-0.46	-1.49	-1.56	-1.13	-0.33	-0.35	-0.67	-0.13
BLX	-2.59	-1.37	-0.78	-0.07	-1.10	-0.42	-1.03	-1.55	-1.55	-0.96	-0.39	-0.60	-0.79	-0.09
TES	-0.74	-1.52	-1.04	-0.35	-1.16	-0.14	-0.78	-0.80	-1.20	-0.73	-0.08	-0.32	-0.76	-0.27
3WF	-1.33	-0.92	-1.10	-0.37	-1.47	-0.31	-0.72	-1.24	-1.48	-0.69	-0.21	-0.35	-0.64	-0.13
DHT	-0.85	-1.36	-0.96	-0.09	-1.24	-0.13	-0.83	-0.95	-1.22	-0.81	-0.19	-0.38	-0.79	-0.20
AS4	-1.59	-1.71	-0.87	-0.20	-1.01	-0.15	-0.95	-1.13	-1.37	-1.16	-0.35	-0.68	-0.93	-0.30
EST	-1.10	-0.86	-1.17	-0.40	-1.45	-0.17	-0.67	-1.17	-1.53	-0.50	-0.11	-0.22	-0.62	-0.16
BM0	-2.05	-1.88	-0.90	-0.13	-1.13	-0.30	-1.07	-1.53	-1.64	-1.10	-0.26	-0.34	-0.70	-0.10
HCY	-1.86	-1.44	-0.76	0.03	-0.86	-0.19	-1.04	-1.11	-1.46	-0.89	-0.37	-0.84	-0.89	-0.12
SNL	-0.58	-2.01	-1.56	-0.15	-1.55	-1.32	-1.09	-1.65	-1.90	-1.26	-0.18	-0.37	-0.72	-0.15
R18	-1.14	-1.24	-1.08	-0.81	-1.47	-0.09	-0.72	-0.92	-1.24	-0.62	-0.09	-0.24	-0.59	-0.21
LE8	-1.29	-1.05	-0.57	-0.01	-0.61	-0.80	-1.95	-0.82	-1.18	-1.28	-0.76	-1.50	-0.70	-0.30
C0R	-1.07	-1.60	-1.01	-0.25	-1.10	-0.10	-1.09	-1.14	-1.33	-1.46	-0.48	-0.58	-0.70	-0.18
1TA	-1.84	-1.59	-0.97	-0.28	-1.05	-0.19	-1.20	-1.86	-1.34	-1.52	-0.38	-0.58	-0.72	-0.25
FLP	-1.88	-1.31	-0.87	-0.11	-0.87	-0.28	-2.13	-0.87	-0.98	-1.47	-0.82	-1.23	-0.81	-0.58
ET0	-0.41	-1.70	-1.12	-0.62	-1.68	-0.64	-0.41	-1.35	-1.47	-0.46	-0.13	-0.09	-0.66	-0.15
MUZ	-0.64	-1.24	-0.86	-0.08	-1.10	-0.45	-1.40	-1.01	-1.21	-0.62	-0.25	-1.03	-0.75	-0.15
GE0	-1.01	-1.40	-1.05	-0.75	-1.72	-0.26	-0.70	-1.02	-1.92	-0.64	-0.17	-0.24	-0.58	-0.36
CA4	-2.15	-1.05	-0.80	-0.01	-0.91	-0.29	-2.03	-0.64	-1.06	-1.00	-0.71	-1.53	-0.99	-0.27
NDR	-1.13	-1.16	-1.01	-0.61	-1.62	-0.18	-0.92	-0.93	-1.31	-0.78	-0.11	-0.29	-0.67	-0.22
STR	-1.17	-1.34	-0.93	-0.22	-1.04	-0.12	-1.00	-0.89	-1.28	-0.71	-0.29	-0.77	-0.85	-0.15
MOF	-1.04	-1.80	-1.14	-0.42	-1.62	-1.52	-1.58	-1.35	-1.55	-0.56	-0.24	-0.93	-0.79	-0.14
MP0	-0.76	-1.19	-0.95	-0.05	-0.95	-0.03	-1.43	-0.93	-1.13	-0.81	-0.21	-0.97	-0.83	-0.14
ND0	-1.45	-1.12	-1.02	-0.60	-1.55	-0.11	-0.95	-0.78	-1.40	-0.97	-0.18	-1.29	-0.87	-0.27
P0M	-0.42	-1.50	-0.97	-0.57	-1.29	-0.20	-0.68	-1.04	-1.57	-0.67	-0.25	-0.71	-0.69	-0.11

Table S3: Per-Residue decomposition of binding energies calculated using MM-PBSA. Ligand binding pocket residues are considered in this analysis. Units are kcal/mol.

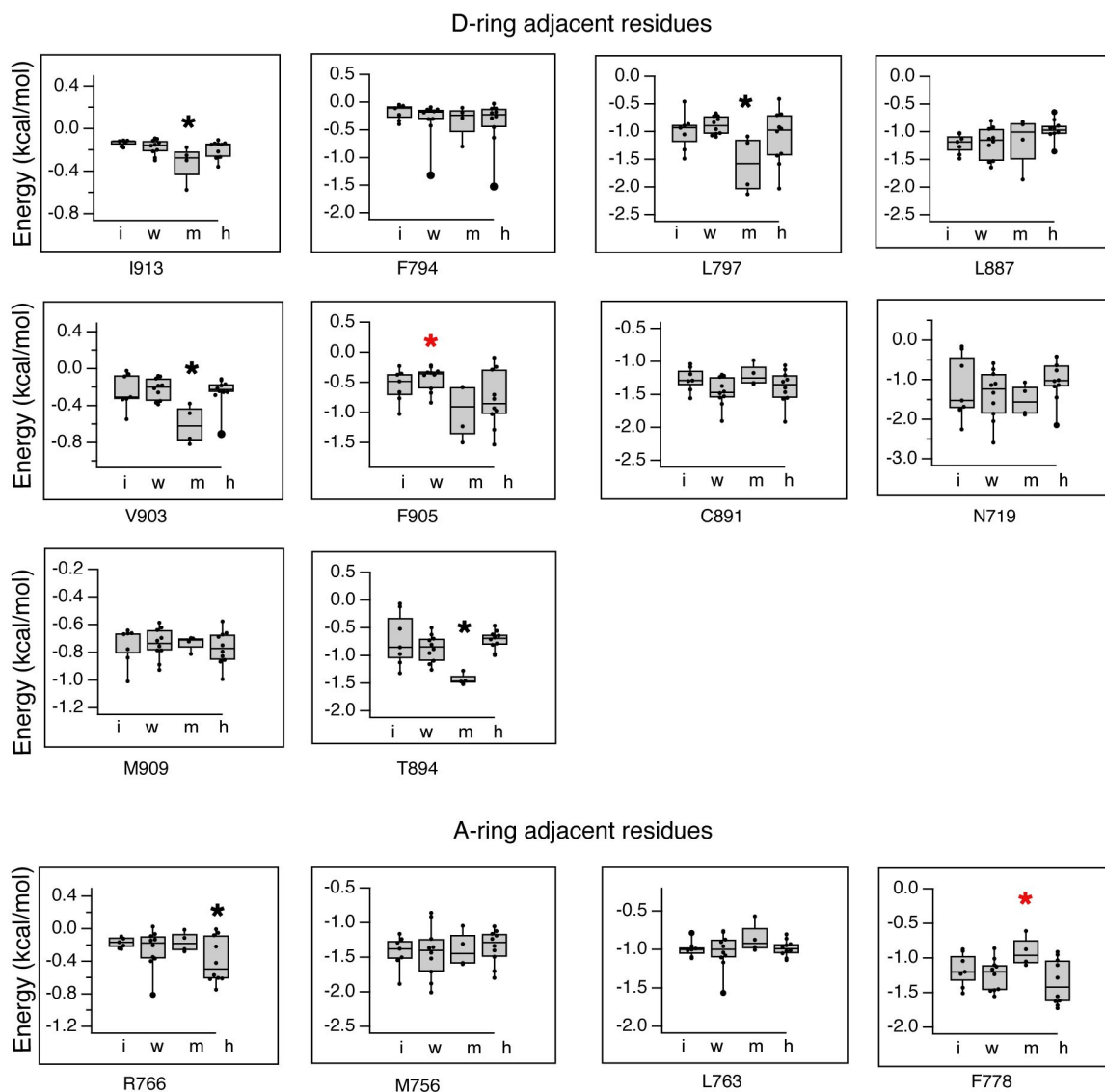


Figure S4. Per-residue decomposition of binding energies calculated by MM-PBSA. Ligand binding pocket residues are considered in this analysis. Values are compared by ligand class and two-tailed unpaired t-tests are used to determine whether energy contributions are significantly lower (black *) or higher (red *) in a given class compared to all other ligands. (significance * is defined as $p < 0.05$).

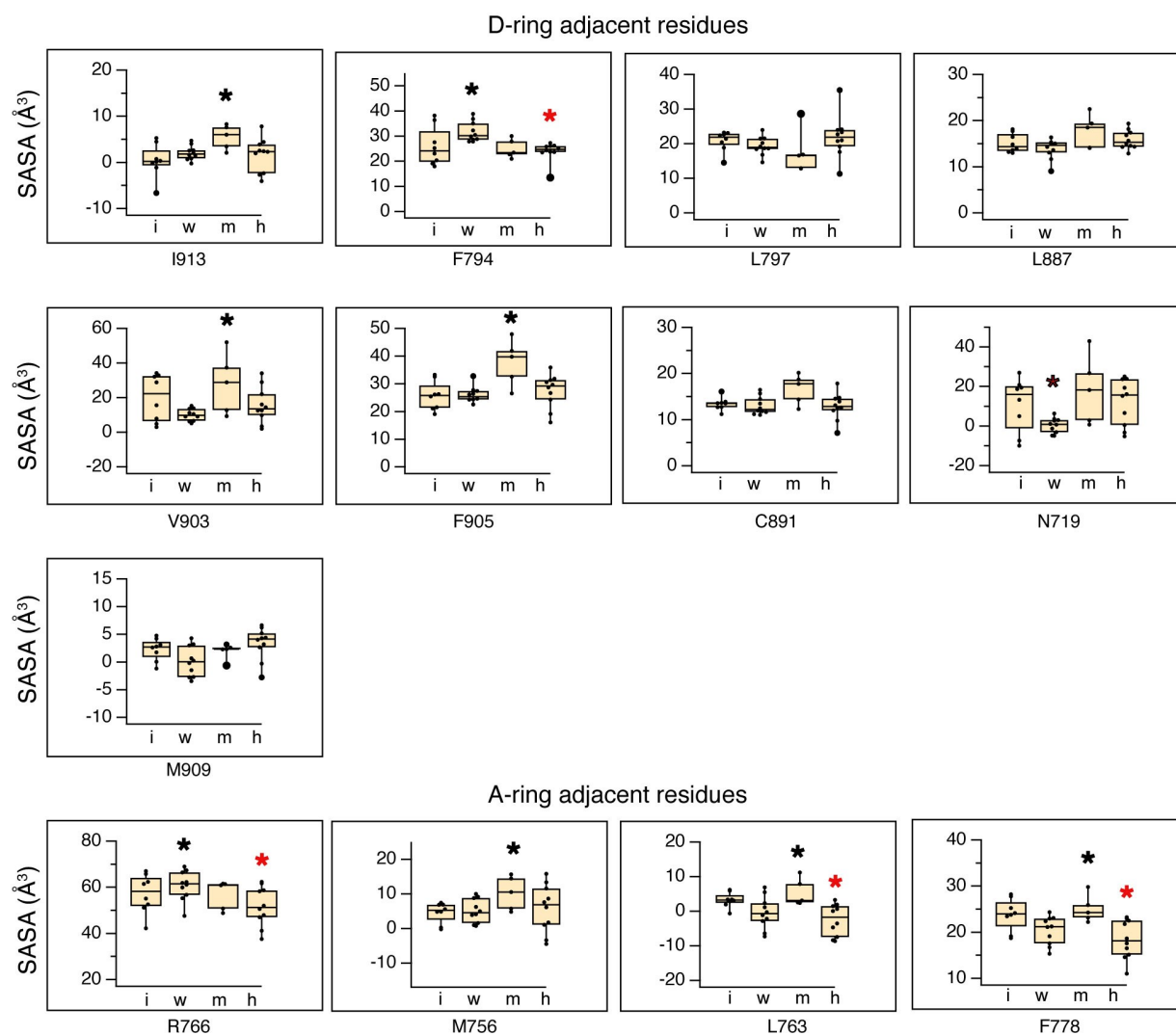


Figure S5. Solvent accessible surface area calculation of binding pocket residues. Ligands are grouped by class (inactive, weak, moderate and high potency). Ligand binding pocket residues are considered in this analysis. Values are compared by ligand class and two-tailed unpaired t-tests are used to determine whether residues in a given class are more exposed (black *) or less exposed (red *) compared to all other ligands. (significance * is defined as $p < 0.05$).

Acceptor residue	atom	Donor residue	atom	Significant class 1			Significant class 2		
				Ligand class (potency)	Direction of significance	Avg occupancy	Ligand class (potency)	Direction of significance	Avg occupancy
E904	O	N719	ND2	weak	high	0.51	moderate	low	0.18
L901	O	S712	OG	weak	high	0.36	moderate	low	0.14
Y777	O	R766	NE	high	high	0.144			
D709	OD1	R788	NE	moderate	high	0.15			
L827	O	R845	NH1	weak	high	0.11	high	low	0.0135
G773	O	W802	NE1	weak	high	0.38			
S793	OG	Y890	OH	weak	high	0.17			
L929	O	R845	NH2	weak	low	0.217			

Table S4. Hydrogen bonds with significant differences in occupancies for individual ligand classes. Eight unique hydrogen bonds were observed in this category. The highest two occupancies were hydrogen bonds between H3 and L11/12. Both had significantly higher occupancy in weak agonists and significantly lower occupancy in moderate potency agonists.

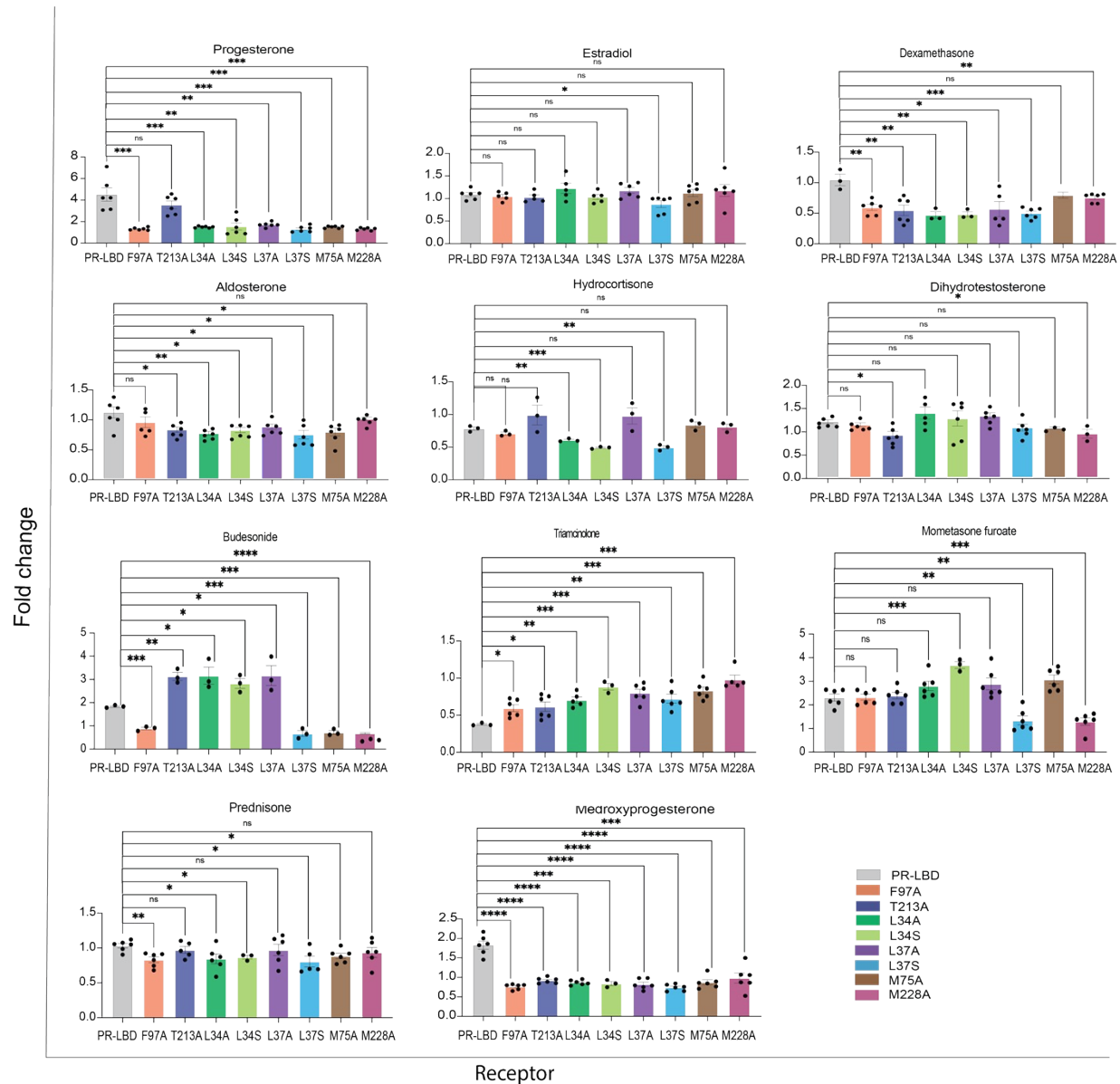


Figure S6: Comparison of the fold activation response of PR-LBD and Mutants at 1 μ M ligand concentration. Residue positions defined with respect to LBD only: F97A (Phe778Ala), T213A (Thr894Ala), M75A (Met756Ala), L34A (Leu715Ala), L34S (Leu34Ser), L37A (Leu718A), L37S (Leu718Ser), M75A (Met756Ala), M228A (Met909Ala).

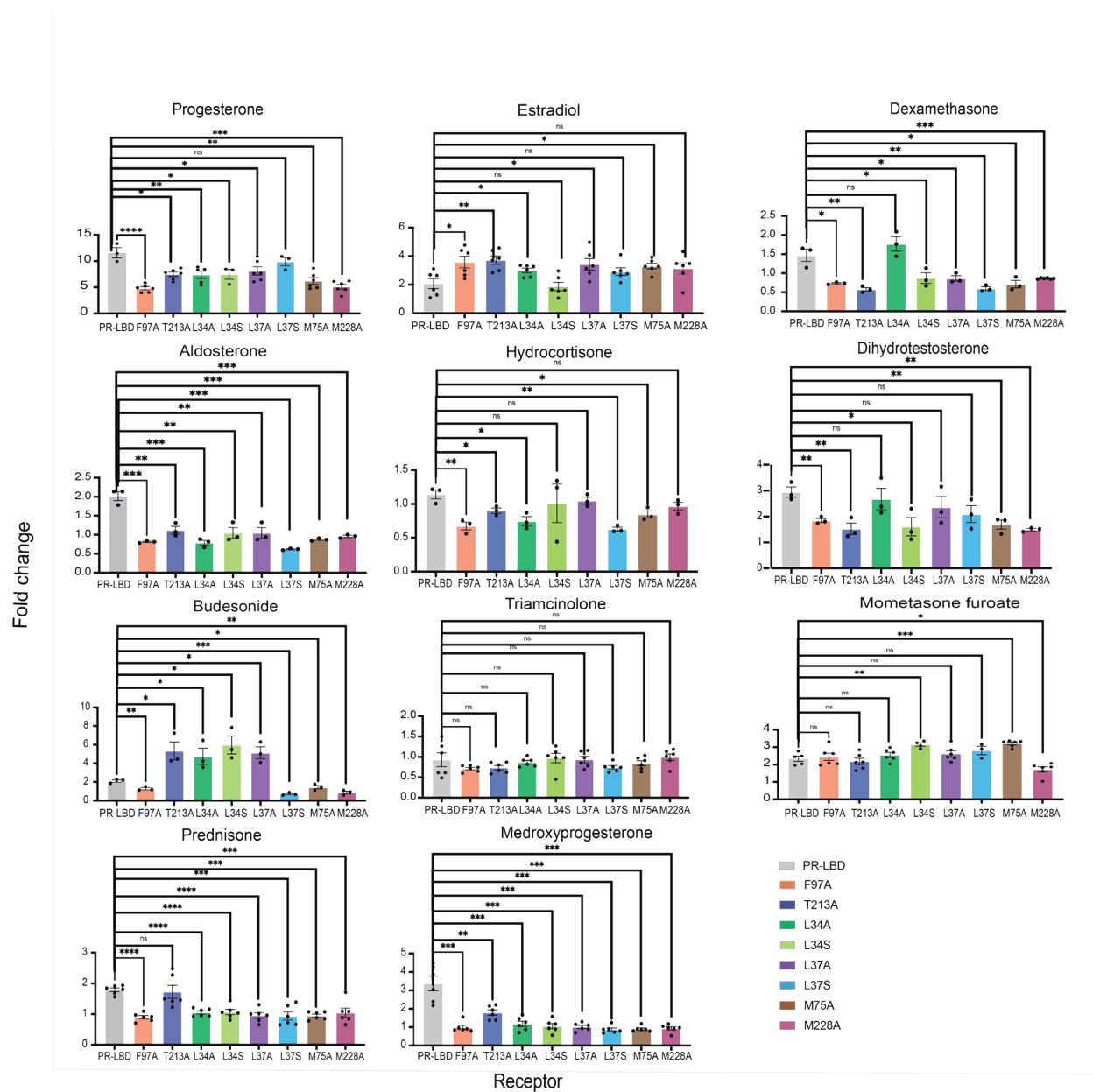


Figure S7: Comparison of the fold activation response of PR-LBD and Mutants at 10 μ M ligand concentration. Residue positions are the same as in Figure S7.

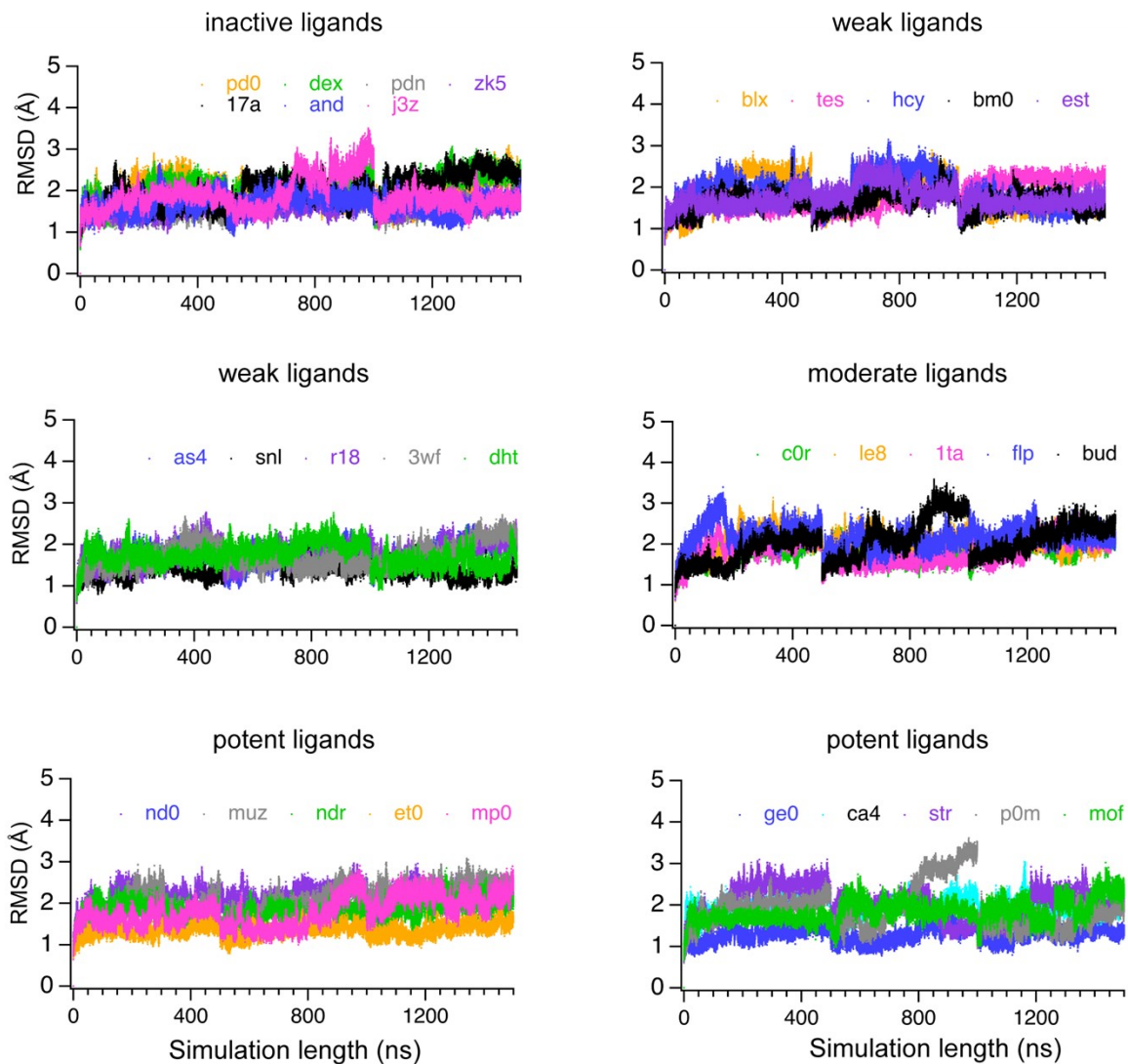


Figure S8. Root mean square deviation (RMSD) plots of all PR complexes. Simulations were performed in triplicate. Each graph represents 3 500-ns segments.